Photomagnetic Nanocomposites

DOI: 10.1002/ange.200802273

Controlled Synthesis of Photomagnetic Nanoparticles of a Prussian Blue Analogue in a Silica Xerogel**

*Giulia Fornasieri and Anne Bleuzen**

Prussian blue and its analogues have attracted much attention over the past decade because of the diversity and tunability of their electronic properties.[1] The possible control of their magnetic properties through external stimuli also makes these compounds good candidates for future molecular memories or switching devices.[2] The successful integration of such functional objects into real applications depends, however, on an additional processing step to control their shape, size, and organization in, or at the surface of, a solid matrix. Several papers in the last few years have discussed the precipitation and characterization of isolated Prussian Blue analogue (PBA) nanoparticles. Different synthetic confining media have been investigated for the precipitation of PBAs, for example reverse micelles,[3] polymers[4] or biopolymer matrixes,[5] ionic liquids,[6] anodic alumina membranes,[7] or mesostructured silica powders.[8] Sol–gel silica shows good optical and mechanical properties, and the mesoporosity of a xerogel can also be used as a confining medium to elaborate PBA nanoparticles. Moore et al., for example, have shown that the simultaneous condensation of silica and CoFe PBA is likely to lead to silica-CoFe PBA nanocomposites.[9] However, as the kinetics of the condensation reactions of silica and CoFe PBA are very different, only carefully controlled synthetic conditions lead to homogeneous nanocomposites. Herein we report the confined precipitation of CoFe PBA nanoparticles in the pores of a silica xerogel. The resulting nanocomposite is homogeneous and exhibits a significant photomagnetic effect. The triggering of the PBA precipitation is fully controlled and completely decorrelated from the silica condensation process, therefore this approach offers new processing perspectives stemming from the exceptional processing flexibility inherent in sol–gel chemistry.

The nanocomposite was obtained by controlled precipitation of CoFe PBA nanoparticles in the pores of a tetraethyl orthosilicate (TEOS) silica xerogel. The elaboration of the nanocomposite involves two distinct condensation processes, namely precipitation of the CoFe PBA and polymerization of silica. Precipitation of the CoFe PBA involves substitution of the water molecules of the hexaaquacobalt(II) ion $[Co^{II}(H_2O)_6]^{2+}$ by $[Fe^{III}(CN)_6]^{3-}$ anions.[10] Given the lability of the hexaaquacobalt(II) complex (the water-exchange rate constant for $[Co^{II}(H_2O)_6]^{2+}$ at 298 K is $3.18\times10^6\ s^{-1}$ [11]), the precipitation of CoFe BPA can be considered as instantaneous. The silica gel is obtained by hydrolysis-condensation of TEOS; both reactions occur by acid- or base-catalyzed bimolecular nucleophilic displacement reactions. The acid catalysis is less effective and produces a polymeric gel with nanometer-sized pores, whereas the basic polymerization is faster but generates a particulate gel with larger pores. The two-step acid/base-catalyzed process is therefore a good compromise to obtain a faster polymerization rate and smaller porosity.[12] The silica polymerization rate is nevertheless still much slower than CoFe PBA precipitation, therefore the direct incorporation of CoFe PBA precursors in a silica sol most often results in phase segregation between the silica gel and the CoFe PBA precipitate (see Figure S1 in the Supporting Information). Confined precipitation of the CoFe PBA in the pores of the matrix is therefore controlled by both condensation processes.

The CoFe PBA precursors were first introduced into the silica matrix prepared by the two-step process separately and characterized in the gel and xerogel phases. Addition of the basic potassium hexacyanoferrate(III) solution to the prehydrolyzed silica sol gave an opaque yellow gel (Figure 2b) due to the precipitation of unmodified $K_3[Fe^{III}(CN)_6]$, which is partially insoluble in the medium. Addition of cobalt(II) nitrate to the prehydrolyzed acidic sol ($pH\approx2$) resulted in a pink coloration of the sol (Figure 1a, left). Subsequent addition of a 2 M aqueous KOH solution to the cobalt(II)-containing sol ($pH\approx9$) was accompanied by an instantaneous color change from pink to deep blue, followed by gelation of the sol (Figure 1a, right). The spectrum of the pink sol shows a multiple band in the visible range assigned to the $^4T_{1g}(F)\rightarrow{}^4T_{1g}(P)$ transition (515 nm) which is the signature absorption of the octahedral $[Co(H_2O)_6]^{2+}$ complex. The spectrum of the deep blue gel shows a strong absorption in the visible range and a multiple band assigned to the $^4A_2\rightarrow{}^4T_1(P)$ energy transition of a Co^{II} ion in a tetrahedral environment. The coordination sphere of the tetrahedral Co^{II} complex in this basic medium is probably composed of hydroxide ligands and anionic SiO^- groups of the silica matrix (see Figure S2 in the Supporting Information). Coordination to the silica matrix is likely to stabilize such tetrahedral species, which are unstable in water and ethanol/water mixtures. The formation of this tetrahedral Co^{II} complex upon increasing the pH of the acidic prehydrolyzed Co^{II}-containing sol is reversible. Thus, acidification of the blue gel makes the gel turn light pink again with

[*] Dr. G. Fornasieri, Prof. A. Bleuzen
Université Paris-Sud, UMR 8182 (ICMMO)
Equipe de Chimie Inorganique
91405 Orsay (France)
Fax: (+33) 1-6915-4754
E-mail: annebleuzen@icmo.u-psud.fr

[**] This research was supported by the French Government through the ANR "Blue Memory" (BLAN06-3_134929). We would also like to thank E. Rivière (ICMMO-ECI) for SQUID measurements and P. Beaunier (Service de microscopie électronique, Université Pierre et Marie Curie) for TEM studies.

Supporting information for this article is available on the WWW under http://dx.doi.org/10.1002/anie.200802273.

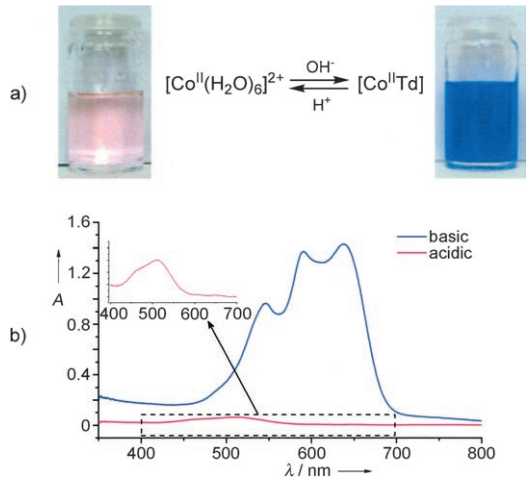

Figure 1. a) Photos of the Co^{II}-containing silica gel in an acidic (left) and basic (right) medium. b) UV/Vis spectra of the Co^{II}-containing silica gel in an acidic (pink) and basic (blue) medium. The dotted region of the spectrum is magnified in the inset.

an absorption spectrum characteristic of the $[Co(H_2O)_6]^{2+}$ complex (see Equation in Figure 1 a).

Addition of a solution of $K_3[Fe^{III}(CN)_6]$ to the blue Co^{II}-containing sol gives a green sol which then gels (Figure 2 c). This gel contains the residual blue tetrahedral Co^{II} complex and hexacyanoferrate(III), as suggested by the color and confirmed by the FTIR absorption band at 2119 cm^{-1}, which corresponds to the stretching vibration of a terminal CN^- anion bonded to Fe^{III}. The stability of the CoFe PBA precursors in the gel, which is probably due to a loss of electrophilicity of the Co^{II} ion and the negative charge borne by the blue basic species, allows the homogeneous insertion of these precursors into the silica matrix. Furthermore, the stability of the CoFe PBA precursors over time allows the condensation of the silica matrix up to the desired polymerization degree as well as further processing steps without PBA formation.

Once the silica network has formed, precipitation of PBA can be triggered simply by acidifying the medium since acidification of the green (xero)gel with an aqueous HNO_3 solution transforms the basic tetrahedral Co^{II} complex into the more reactive cationic $[Co^{II}(H_2O)_6]^{2+}$ complex. Reaction of the hexaaquacobalt(II) complex with hexacyanoferrate(III) to give the CoFe PBA is accompanied by an instantaneous color change of the gel or xerogel (Figure 2 d). The presence of a large excess of Rb^+ cations in the HNO_3 solution leads to the formation of a violet rubidium CoFe PBA containing a significant amount of alkali-metal cations that essentially consists of Co^{III}–Fe^{II} diamagnetic pairs.[10] The IR spectrum of the nanocomposite confirms this composition. Thus, in addition to the signals of the silica matrix, a broad absorption band centered at 2125 cm^{-1} (Figure 2 e). This signal can be attributed to the stretching vibrations of a cyanide anion in an Fe^{II}–CN–Co^{III} environment. The X-ray powder diffraction pattern confirms the face centered cubic structure (see Figure S3 in the Supporting Information) of this PBA. The cell parameter value ((9.97 ± 0.05) Å) is compatible with a majority of low-spin Co^{III} ions.[10] The violet nanocomposite therefore consists of a silica matrix containing a maximum of 1.8 % of Rb–CoFe PBA, which corresponds to 1.1 mol % total-metal to silicon (Rb + Co + Fe/Si). Silica confines the precipitation of the PBA to such an extent that it forms as dispersed nanoparticles, as shown by TEM measurements of microtomed samples (Figure 3). These nanoparticles ((40 ± 12) nm in diameter) form by the assembly of several crystallographic domains, each of about 8 nm, as supported by high-magnification TEM images (see Figure S4 in the Supporting Information).

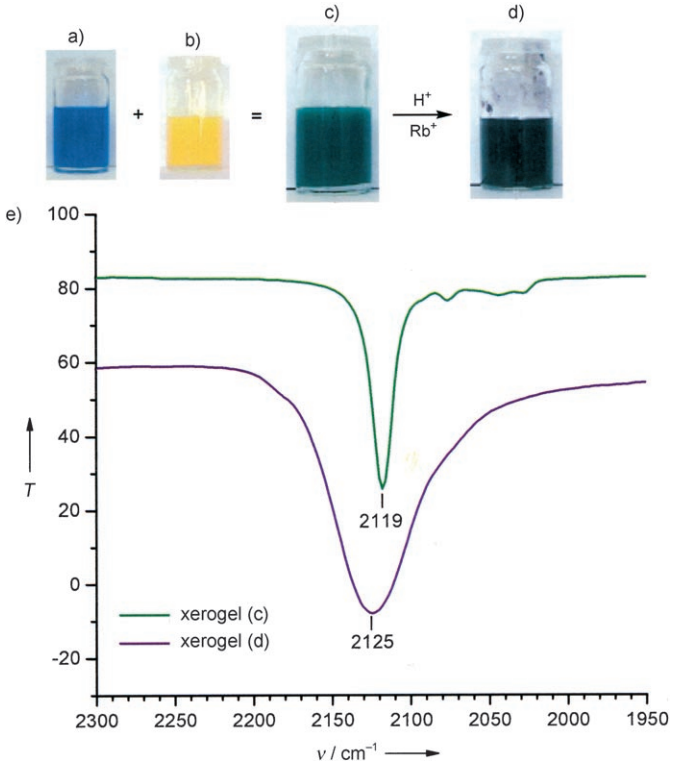

Figure 2. Photos of a) the Co^{II}-containing silica sol in a basic medium, b) the $[Fe^{III}(CN)_6]^{3-}$-containing silica sol, c) the Co^{II}-containing silica sol in a basic medium after addition of $[Fe^{III}(CN)_6]^{3-}$, d) the Rb–CoFe PBA-silica nanocomposite, and e) the FTIR spectra of the xerogels prepared from the sols in (c) and (d).

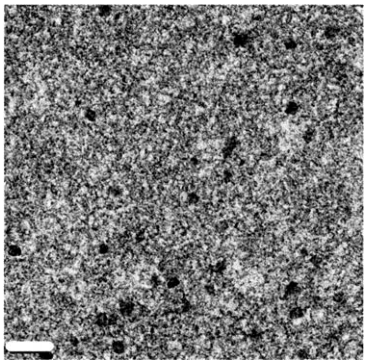

Figure 3. A TEM image of the Rb–CoFe PBA-silica nanocomposite xerogel (microtomed sample). The scale bar is 100 nm.

The bulk Rb–CoFe PBA shows a remarkable photomagnetic effect at low temperature.[10] Thus, irradiation of the compound with visible light at low temperature results in an electron transfer that transforms the Co^{III}–Fe^{II} diamagnetic pairs into Co^{II}–Fe^{III} paramagnetic pairs with a net increase of the magnetization of the material. This transformation can be reversed by heating above the relaxation temperature (about 110 K). An analogous photomagnetic effect was also verified for our nanocomposite (Figure 4). Thus, irradiation of the Rb-CoFe PBA silica nanocomposite with a green laser results in an increase in magnetization, which can be erased by heating up to 110 K. This phenomenon is observable with a 4-mg sample containing only 72 μg of Rb–CoFe PBA nanoparticles. The bulk compound shows ferrimagnetic behavior, with a T_c of 21 K, after irradiation.[10] This magnetic ordering temperature is not detectable for the Rb–CoFe PBA silica nanocomposite, probably because of the nanometric size of the crystallographic domains.

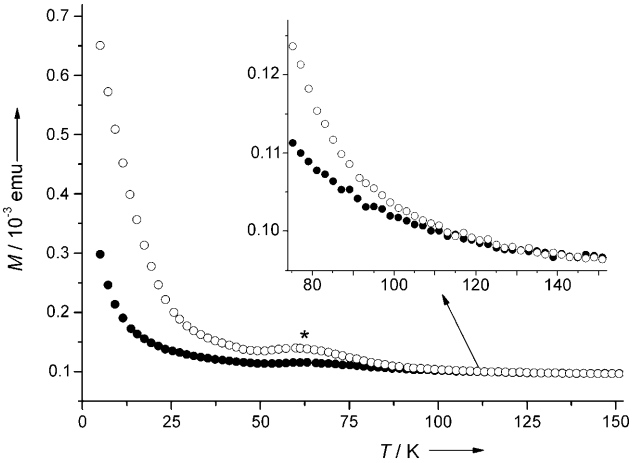

Figure 4. Field-cooled magnetization curves for the Rb–CoFe PBA-silica nanocomposite before (●) and after (○) irradiation at $H = 5000$ Oe. The feature marked with an asterisk corresponds to the contribution of O_2 adsorbed in the pores of the silica nanocomposite. The inset shows an enlargement of the thermal relaxation zone.

In conclusion, this original process, which involves a reversible protection of Co^{II} ions, allows the confined precipitation of Rb–CoFe PBA in the pores of a silica xerogel. This nanocomposite exhibits a significant photomagnetic effect, and this approach could offer new processing perspectives for the development of information storage devices. Work is currently in progress to control the size and the organization of the PBA particles in bulk and thin film nanocomposites.

Experimental Section

The silica gel was prepared by a two-step hydrolysis process, the first step of which involves mixing tetraethyl orthosilicate (8.6 mL, 38.4 mmol), ethanol (6.8 mL), water (0.7 mL, 38.4 mmol), and 37% nitric acid (1 μL) at 60 °C. After stirring for 1.5 h, cobalt(II) nitrate hexahydrate (0.16 mmol) was solubilized in the sol at room temperature, whereupon the sol became pink. An aqueous KOH solution (2 M) was then added in two fractions (0.87 mL of 2 M KOH, followed by 0.87 mL of 2 M KOH containing 0.16 mmol of potassium hexacyanoferrate(III)) for the second hydrolysis step. The green sol gelled in 30 s. This gel was aged in a sealed vial for one week and dried at room temperature for one week after being coarsely ground.

The green xerogel was dispersed in 30 mL of an acidic rubidium nitrate solution (2.42 mmol of $RbNO_3$ in 0.6% HNO_3), whereupon the rubidium Co-Fe PBA precipitated in the silica matrix to give a violet nanocomposite. The final product was washed three times with water to eliminate residual ions and recovered by centrifugation after each washing.

Received: May 15, 2008
Published online: September 2, 2008

Keywords: cobalt · confined precipitation · nanostructures · Prussian Blue · sol–gel processes

[1] a) M. Verdaguer, G. Girolami in *Magnetism: Molecules to Materials* (Eds.: J. S. Miller, M. Drillon), Wiley-VCH, Weinheim, **2005**; b) S.-I. Ohkoshi, K. Hashimoto, *Electrochem. Soc. Interface* **2002**, *11*, 34–38.
[2] a) O. Sato, T. Iyoda, A. Fujishima, K. Hashimoto, *Science* **1996**, *272*, 704–705; b) S.-I. Ohkoshi, K. Hashimoto, *J. Photochem. Photobiol. C* **2001**, *2*, 71–88; c) A. Dei, *Angew. Chem.* **2005**, *117*, 1184–1187; *Angew. Chem. Int. Ed.* **2005**, *44*, 1160–1163.
[3] a) S. Vaucher, J. Fielden, M. Li, E. Dujardin, S. Mann, *Nano Lett.* **2002**, *2*, 225–229; b) L. Catala, T. Gacoin, J.-P. Boilot, E. Rivière, C. Paulsen, E. Lhotel, T. Mallah, *Adv. Mater.* **2003**, *15*, 826–829.
[4] a) T. Uemura, M. Ohba, S. Kitagawa, *Inorg. Chem.* **2004**, *43*, 7339–7345; b) L. Catala, A. Gloter, O. Stephan, G. Rogez, T. Mallah, *Chem. Commun.* **2006**, 1018–1020.
[5] a) N. Gálvez, P. Sánchez, J. M. Domínguez-Vera, *Dalton Trans.* **2005**, 2492–2494; b) Y. Guari, J. Larionova, K. Molvinger, B. Folch, C. Guerin, *Chem. Commun.* **2006**, 2613–2615.
[6] G. Clavel, J. Larionova, Y. Guari, C. Guérin, *Chem. Eur. J.* **2006**, *12*, 3798–3804.
[7] A. Johansson, E. Widenkvist, J. Lu, M. Boman, U. Jansson, *Nano Lett.* **2005**, *5*, 1603–1606.
[8] a) G. Clavel, Y. Guari, J. Larionova, C. Guerin, *New J. Chem.* **2005**, *29*, 275–279; b) B. Folch, Y. Guari, J. Larionova, C. Luna, C. Sangregorio, C. Innocenti, A. Caneschi, C. Guerin, *New J. Chem.* **2008**, *32*, 273–282.
[9] J. G. Moore, E. J. Lochner, C. Ramsey, N. S. Dalal, A. E. Stiegman, *Angew. Chem.* **2003**, *115*, 2847–2849; *Angew. Chem. Int. Ed.* **2003**, *42*, 2741–2743.
[10] A. Bleuzen, C. Lomenech, V. Escax, F. Villain, F. Varret, C. Cartier dit Moulin, M. Verdaguer, *J. Am. Chem. Soc.* **2000**, *122*, 6648–6652.
[11] Y. Ducommun, K. E. Newman, A. E. Merbach, *Inorg. Chem.* **1980**, *19*, 3696–3703.
[12] C. J. Brinker, G. W. Scherer, *Sol-Gel Science*, Academic Press, San Diego, **1990**, pp. 515–615.

